ChemPubSoc Europe

DOI: 10.1002/cbic.201600302

CHEMBIOCHEM Full Papers

Cationic DOPC–Detergent Conjugates for Safe and Efficient in Vitro and in Vivo Nucleic Acid Delivery

Philippe Pierrat,[a] Anne Casset,[a] Pascal Didier,[b] Dimitri Kereselidze,[a] Marie Lux,[a] Françoise Pons,[a] and Luc Lebeau*[a]

The ability of a nonviral nucleic acid carrier to deliver its cargo to cells with low associated toxicity is a critical issue for clinical applications of gene therapy. We describe biodegradable cationic DOPC–$C_{12}E_4$ conjugates in which transfection efficiency is based on a Trojan horse strategy. In situ production of the detergent compound $C_{12}E_4$ through conjugate hydrolysis within the acidic endosome compartment was expected to promote endosome membrane destabilization and subsequent release of the lipoplexes into cytosol. The transfection efficiency of the conjugates has been assessed in vitro, and associated cytotoxicity was determined. Cellular uptake and intracellular distribution of the lipoplexes have been investigated. The results show that direct conjugation of DOPC with $C_{12}E_4$ produces a versatile carrier that can deliver both DNA and siRNA to cells in vitro with high efficiency and low cytotoxicity. SAR studies suggest that this compound might represent a reasonable compromise between the membrane activity of the released detergent and susceptibility of the conjugate to degradation enzymes in vitro. Although biodegradability of the conjugates had low impact on carrier efficiency in vitro, it proved critical in vivo. Significant improvement of transgene expression was obtained in the mouse lung tuning biodegradability of the carrier. Importantly, this also allowed reduction of the inflammatory response that invariably characterizes cationic-lipid-mediated gene transfer in animals.

Introduction

Gene therapy is an experimental approach that uses genes or other nucleic acids (oligonucleotides, siRNA…) to treat or prevent diseases. It involves intracellular delivery of a therapeutic nucleic acid with full functional integrity so it becomes available to the cellular machinery for proper processing and action. Because of the anionic nature both of the plasma cell membrane and of nucleic acids, intracellular delivery of the latter requires the use of a safe and efficient vector, and this definitely represents one of the greatest technical challenges in modern medicine. Thus, although potent viral vectors have been developed, gene therapy has seen only limited success to date, primarily due to safety concerns.[1] Additional limitations with viral vectors reside in the maximum size of the DNA fragments they can package (< 5 Kbp),[2] in difficulties met in large-scale preparation,[3] and in production costs.[4]

As an alternative to viral vectors, synthetic carriers have attracted much attention from chemists.[5] In particular, a large number of cationic lipids have been developed, and their huge potential for intracellular delivery of nucleic acids has been demonstrated. However, after more than 20 years of intensive research, few clear conclusions have emerged on the relationships between the structures and compositions of lipidic carriers and the transfection efficiencies and safety of the lipoplexes made from them.[6] Furthermore, most of those nonviral carriers that proved effective for delivering nucleic acids in vitro either failed to deliver their cargoes in vivo or induced unacceptable associated toxicity. Therefore, there is still a pressing need to develop synthetic vectors offering a full guarantee of efficiency and safety, to pave the way for therapeutic applications and to translate gene therapy into a reality.

Intracellular gene delivery by cationic lipids is a complex process.[7] Cationic lipid/nucleic acid complexes—that is, lipoplexes—are formed through electrostatic interaction between the cationic head groups of the lipids and the anionic phosphates in nucleic acids, the hydrophobic part of the lipids driving the condensation of the complexes into discrete particles by a spontaneous self-assembly process. It is widely accepted that cationic lipoplexes prepared with an excess of cationic lipid attach to negatively charged cell-surface proteoglycans.[8] After cell binding, lipoplexes enter the cells primarily by endocytosis. Most particles remain trapped in the endosome, and undergo degradation upon fusion of matured endosome with lysosomes.[9] Lipoplexes that succeed in endosome escape dissociate in the cytosol, and their DNA can migrate toward the nucleus, under threat of degradation by nucleases, for nuclear import and proper processing.

[a] Dr. P. Pierrat, Dr. A. Casset, D. Kereselidze, M. Lux, Prof. F. Pons, Dr. L. Lebeau
Laboratoire de Conception et Application de Molécules Bioactives
UMR 7199 CNRS–Université de Strasbourg, Faculté de Pharmacie
74 route du Rhin, B.P. 60024, 67401 Illkirch (France)
E-mail: llebeau@unistra.fr

[b] Dr. P. Didier
Laboratoire de Biophotonique et Pharmacologie
UMR 7213 CNRS–Université de Strasbourg, Faculté de Pharmacie
74 route du Rhin, B.P. 60024, 67401 Illkirch (France)

Supporting information for this article can be found under http://dx.doi.org/10.1002/cbic.201600302.

Every one of these steps is challenging and can severely hinder transfection efficiency. Endosome escape is probably the most critical, and many efforts have been devoted to the development of nucleic acid delivery systems with specific endosome-membrane-disrupting properties. Inclusion of the helper lipid 1,2-dioleoyl-*sn*-glycero-3-phosphoethanolamine (DOPE) into the DNA complexes was shown to improve endosome escape.[10] The effect presumably relies on the ability of DOPE to induce destabilization of the endosomal membrane by lipid phase transition to the inverted hexagonal phase. Incorporation of pH-sensitive lipids in the lipoplexes gave similar results. These form stable lipid bilayers at physiological pH (pH 7.4) but undergo membrane destabilization under acidic conditions (e.g., in late endosome).[11] Membrane-active peptides presenting small amphipathic domains also proved efficient in facilitating endosome escape.[12]

The use of detergents for gene delivery applications, in order to improve endosome escape and transfection efficiency, has been considered as well.[13] However, this approach has achieved only limited success. Indeed, as a consequence of the high critical micellar concentrations (CMCs) of detergents, a rapid depletion of these amphiphilic molecules from the transfection particles occurs upon dilution in biological media, provoking premature decondensation of the nucleic acid and thus precluding its internalization by the cells.

Recently, the use of cationic lipids resulting from the conjugation of Triton X-100, a surfactant with high membrane-solubilizing potential, with the endogenous membrane phospholipid 1,2-dioleoyl-*sn*-glycero-3-phosphocholine (DOPC) for nucleic acid intracellular delivery has been described.[14] Conjugation was performed with the aid of various acetal linkers, in such a way that these lipids can lose their cationic charge upon hydrolysis upon either a chemical or an enzymatic stimulus.[15] Biodegradation of the conjugates—inside the acidic endosomal compartment or upon exposure to lysosomal enzymes, for example—results in production of Triton X-100 and DOPC. This has several advantages: 1) intracellular accumulation of potentially toxic cationic species[16] is avoided, 2) detergent produced in situ can destabilize the endosome membrane, thus improving the escape of the entrapped genetic material into the cytoplasm, and 3) as a zwitterionic species, DOPC cannot maintain the integrity of the lipoplexes, and this results in the decondensation of the nucleic acid payload, which thus becomes available to the cell machinery for processing. High in vitro transfection efficiency was achieved with these biodegradable DOPC–detergent conjugates but this came with significant associated cytotoxicity, most likely due to intrinsic toxicity of the detergent released in situ.

The intrinsic toxicity profiles of nucleic acid carriers might be a barrier to in vivo applications. We believed that changing the structure of the detergent in the previous conjugates might have beneficial effects on the transfection process. Especially, we had it in mind to improve the efficacy of this Trojan horse strategy by placing endosome escape under the control of the detergent species generated in situ, and managing the associated toxicity. We thus considered *n*-dodecyl tetra(ethylene glycol) ether ($C_{12}E_4$), which is known to be a soft detergent with acceptable biocompatibility.[17] This detergent was conjugated to DOPC in various ways (Scheme 1). The resulting conjugates were subjected to evaluation of their properties in terms of nucleic acid condensation and of the sizes and charges of the resulting particles. Their efficacy in mediating intracellular DNA and siRNA delivery and their associated cytotoxicity were assessed on various cultured cell lines. Cellular uptake, intracellular distribution, and intracellular disassembly of the lipoplexes were examined by fluorescence techniques. Finally, preliminary experiments involving gene delivery to the mouse lung were performed to determine whether and how the results obtained in vitro could translate in vivo.

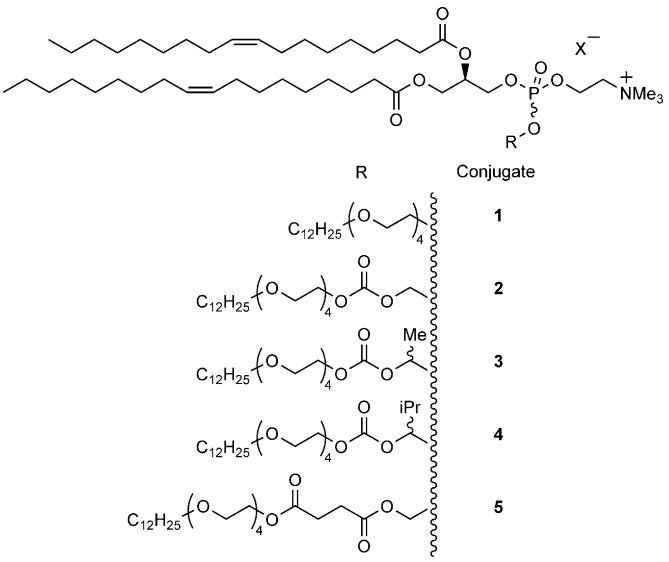

Scheme 1. Structures of the investigated DOPC–detergent conjugates.

Results and Discussion

Synthesis of the cationic DOPC–detergent conjugates

Preparation of compound **1** was achieved as previously described.[18] Briefly, $C_{12}E_4$ (**7**) was prepared from 1-bromododecane and tetra(ethylene glycol) in 50% aqueous sodium hydroxide, and transformed into the corresponding trifluoromethanesulfonyl ester **8** (Scheme 2). The compound was unstable,

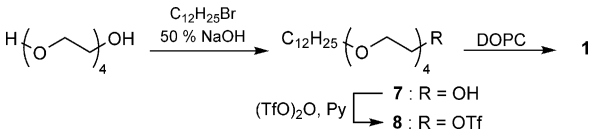

Scheme 2. Synthesis of the cationic DOPC–detergent conjugate **1**.

and decomposition occurred on standing at room temperature in chloroform. Analysis of degradation products was consistent with a deoligomerization process leading to the formation of dioxane as reported previously with other activated poly(ethylene glycol) (PEG) derivatives.[19] Consequently, compound **8**

was directly subjected to nucleophilic displacement by DOPC to form conjugate **1**, obtained as a mixture of two diastereomers (53% yield).

Conjugates **2**–**4** were prepared as described in Scheme 3. $C_{12}E_4$ was acylated with various 1-chloroalkyl chloroformates to provide chloromethyl carbonates **9**–**11** in 92–96% yield. Treatment of these intermediates with DOPC directly provided the expected conjugates **2**–**4** in 20–37% yield. Conjugate **5** was obtained through standard acylation of $C_{12}E_4$ with succinic anhydride. The resulting hemisuccinate **12** was then treated with chloromethyl chlorosulfate to provide the corresponding chloromethyl ester **13** quantitatively. Treatment of **13** with DOPC led to conjugate **5** in 21% yield.

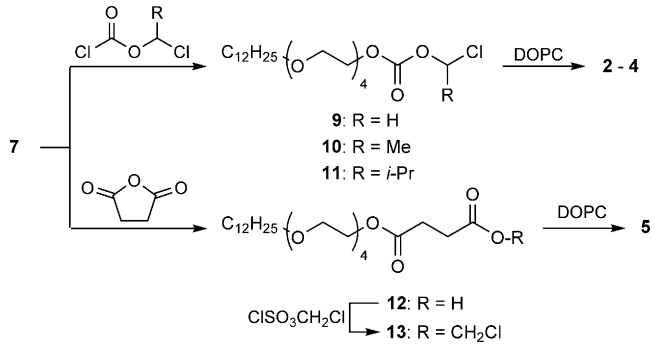

Scheme 3. Synthesis of the cationic DOPC–detergent conjugates **2**–**5**.

Preparation and characterization of lipoplexes

The ability of cationic lipids **1**–**5** to interact electrostatically with nucleic acids and form lipoplexes was determined by a conventional electrophoretic retardation assay (Figure S1 in the Supporting Information). It was observed that the nature of the substituent introduced at the phosphate group of DOPC had no adverse effect on the ability of the ammonium polar head of the cationic lipid to interact with phosphates in the nucleic acid backbone. All conjugates fully retarded nucleic acid at *N*/*P* values between 0.8 and 1.0 (where *N* is the concentration of the lipid ammonium group and *P* that of nucleic acid phosphates), except for conjugate **4**. In that case, a higher *N*/*P* charge ratio was required for full condensation of nucleic acid ($N/P > 1.5$). The sizes and ζ potentials of the complexes prepared with DNA and siRNA were systematically determined by dynamic light scattering (DLS) measurements. The data are presented in the Supporting Information (Tables S1 and S2) and are specifically referred to in the following discussion.

Hydrolytic stability of the DOPC–detergent conjugates

Compounds **1**–**5** were designed in order to display various susceptibilities towards hydrolysis, due to the presence of an acetal moiety connecting DOPC to the detergent species, hopefully with various rates of detergent release in biological media. Thus, their hydrolytic stability was first determined in vitro under neutral and acidic conditions, according to a previously described procedure.[15] Briefly, the conjugates were formulated into liposomes by use of an injection technique,[20] in buffered saline at pH 7.4 and 4.5, and incubated at 37 °C. ^{31}P NMR titration of starting material (phosphotriester) against DOPC (phosphodiester) allowed determination of the time, $t_{1/2}$, required for 50% hydrolysis (Table 1). As might be expected,

Table 1. Hydrolytic stability of conjugates **1**–**5**. Compounds formulated into liposomes were incubated at 37 °C, and hydrolysis was monitored by ^{31}P NMR measurements. The time required for 50% hydrolysis ($t_{1/2}$) was calculated from theoretical curve fitting with the experimental data.

	$t_{1/2}$ [h]				
	1	**2**	**3**	**4**	**5**
pH 4.5	–[a]	234	13.6	84	148
pH 7.5	–[a]	48	16.5	107	92

[a] No hydrolysis could be detected after an incubation period of seven days.

incubation of conjugate **1** did not result in any formation of DOPC or other degradation product, even over an extended period of time (seven days). Conjugates **3** and **4**, each bearing an alkyl substituent on the acetal bridge, exhibited hydrolytic susceptibility that was exacerbated at low pH, as was anticipated in view of the presence of the acetal bridge. However, and this is contrary to our first expectations, conjugates **2** and **5** did not follow this trend and were more rapidly hydrolyzed under slightly alkaline conditions. This might find an explanation in that the hydrolytic stability of the conjugates is the result of a delicate balance between the sensitivity of the acetal bridge under acidic conditions and that of the carbonate or ester groups under acidic and basic conditions. It also depends on the hydration state of the polar head of the conjugates. Depending on the reaction mechanism (specific base-catalyzed, water-catalyzed, or specific acid-catalyzed), the hydrolysis of carbonate and ester within the conjugates proceeds at various rates as they are altered by the inductive and steric properties of the substituent groups.[21] Furthermore, combination of these functional groups with phosphate and acetal moieties within the same molecular scaffold might possibly allow for intramolecular catalysis. As a consequence, further interpretation of the results in Table 1 remains difficult and would require hydrolysis data obtained with additional conjugates for precise determination of the influence of each functional group on the overall (in)stability of the compounds.

In vitro transfection efficiency and cytotoxicity of the DOPC–detergent conjugate/DNA complexes

The ability of the DOPC–detergent conjugates to mediate DNA delivery in cells was determined by measuring the levels of transgene expression in various cell lines incubated with lipoplexes (Figure 1, left). Lipoplexes were prepared with the pCMV-FLuc DNA plasmid at three different *N*/*P* charge ratios (1, 3, and 5), in the presence of 10% fetal bovine serum (FBS). The cytotoxicity of the formulations was determined in parallel, by using a lactate dehydrogenase (LDH) cell release assay

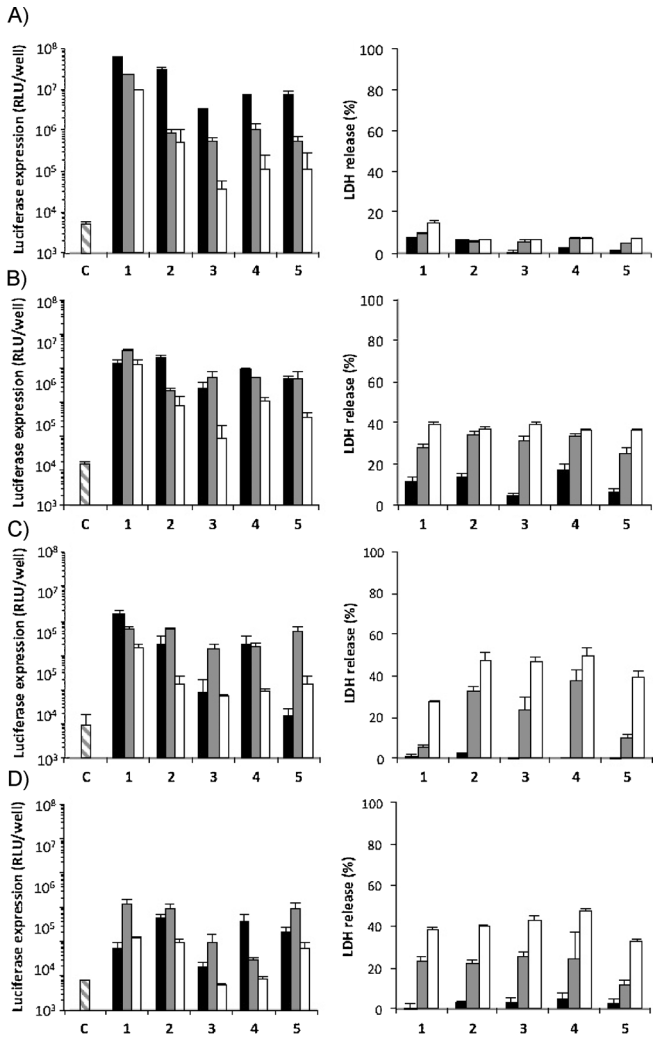

Figure 1. Expression of luciferase (left) and LDH release (right) in A) BHK-21, B) NCI-H292, C) A549, and D) Calu-3 cells treated for 24 h with pCMV-FLuc complexed with conjugates **1**–**5**, at various *N*/*P* ratios [1 (black), 3 (gray), 5 (white)], in the presence of 10% FBS. "**C**" (control) refers to untreated cells.

(Figure 1, right). Firstly, DNA complexes with conjugates **1**–**5** were quite similar with respect to their size and ζ potentials (Table S1). This was probably a result of the high structural homogeneity within the investigated conjugate series. Next, the transfection rates, as measured by the production of the firefly luciferase protein, were highly dependent on the cell line investigated. Thus, BHK-21 cells were transfected at the higher rate, whereas NCI-H292 and A549 cells were less affected, by an order of magnitude. Calu-3 cells proved more difficult to transfect. This was probably related to their capacity to secrete mucus, which constitutes an additional obstacle to penetration of cells by transfection particles. Furthermore, it transpired that the transfection rates were strongly influenced by the *N*/*P* charge ratios for the more labile conjugates **2**–**5**, whereas smaller variations were observed with compound **1**. Remarkably, higher transfection rates were regularly obtained at the *N*/*P* charge ratio of 1, for which the lipoplexes displayed negative ζ potential values (Table S1). This provides evidence that there is no need for the particles to be positively charged in order to interact with the negatively charged cell membrane, and to trigger cellular uptake. As a matter of fact, in the serum-containing cell culture medium, serum proteins compete for the nanoparticle surface, leading to the formation of a protein corona that largely defines the biological identity of the nanoparticle.[22] Whatever the charge of the nanoparticle, this process occurs within minutes[23] and hence is compatible with the timing of the incubation process in the transfection experiments.

Considering each cell line separately and regardless of the *N*/*P* ratio, higher transfection efficiency was invariably achieved with conjugate **1**, except in the case of the difficult to transfect Calu-3 cell line, for which mixed results were obtained. Although this set of data allows several alternative interpretations, it seems clear that the introduction of a sensitive connector within the structure of the conjugate is detrimental to its DNA delivery efficiency in vitro. The hydrolytic susceptibilities of the conjugates as measured in buffered saline (Table 1) did not reflect the situation encountered in the biological media and underestimated the degradation rates of the conjugates. Indeed, in such an environment, chemical transformations are mostly under the control of enzymes, with high catalytic turnover and reaction rates that cannot be matched under acid/base-catalyzed conditions. As a corollary, the more labile conjugates might not be stable enough to enzymes to allow effective delivery of DNA to cells, either because they cannot maintain the integrity of the transfection particles until they enter cells, or because premature intracellular DNA decondensation makes diffusion to the nucleus more difficult and exposes the nucleic acids to nucleases en route.

With respect to cytotoxicity, the labile conjugates proved less harmful to cells than compound **1**, at least in the case of the easy to transfect BHK-21 cell line. With the other cell lines, results were not as clear-cut. At optimum charge ratio ($N/P = 1$), almost negligible membrane damage was observed because the amount of LDH released by cells was below 5–10%, except in the case of the NCI-H292 cells. At higher charge ratio, a significant and predictable increase in LDH release was measured. Indeed, the more cationic the particles, the greater their propensity to engage in direct fusion with the negatively charged plasma membrane. Although membrane fusion can be non-leaky, it is very common to lose material from the vesicle interior during the later stages of membrane unification, as has been shown with, for example, synthetic liposomes[24] and lysosomes.[25] It is worth noting that fusion of lipoplexes with the plasma membrane need not necessarily translate into cellular uptake of the plasmid DNA and subsequent transgene expression. Most probably, the DNA molecules remain trapped onto the outer leaflet of the plasma membrane, similarly to what has previously been reported for lipoplexes prepared with cationic surfactants.[26] Lastly, improving the charge ratio was invariably associated with cytotoxicity; this is consistent with higher intracellular concentration of the toxic cationic species, but suggests that the internalized material was only poorly released into the cytosol for correct transgene expression. Additional data on cytotoxicity of the carriers alone can be found in the Supporting Information (Figure S2).

Cellular uptake and intracellular distribution of the lipoplexes

Cellular uptake of the lipoplexes was investigated by flow cytometry. BHK-21 cells were incubated with lipoplexes prepared with Cy5-labeled DNA and collected at 4 h for analysis. The cyanine dye was excited at 640 nm, and fluorescence was measured at 660 nm. With regard to the percentage of Cy5-positive cells (i.e., cells that internalized lipoplexes), all the conjugates achieved high scores (>85%), except for conjugate **4** (51%; Figure 2A). The differences between the compounds were amplified on examination of the mean fluorescence intensities of the cells (Figure 2B). Thus, a higher rate of DNA internalization was obtained with conjugate **2**, whereas **4** appeared to be a less effective carrier in the series with a reduction of DNA cellular uptake by more than an order of magnitude. These conclusions, however, must be tempered because the data are only semiquantitative, due to Cy5 fluorescence self-quenching within the transfection particles (Figure S3). Indeed, in the condensed Cy5-labeled DNA particles, the local concentration of the cyanine dye is significantly improved so the distance between two neighboring dye units allows cross-relaxation, as has already been reported with other fluorophore-labeled DNA complexes.[27] Thus, disaggregation of the labeled lipoplexes inside cells comes with fluorescence dequenching and makes accurate quantitative analysis difficult, if not impossible. Moreover, the fluorescence data cannot be directly correlated with transfection efficiency, because they give a picture of the situation at time point 4 h, whereas transfection was measured 20 h later. Furthermore, quantification of cellular uptake provides no information on intracellular processing of the lipoplexes, which would be expected to be variable depending on the stability of the carrier in the cellular compartment. Notably, lipoplexes prepared with compound **4** were poorly internalized by cells but led to high transgene expression, revealing that they were processed inside the cells in more timely manner than other lipoplexes, with regard to, for example, their escape from the endosome and DNA decondensation, degradation by nucleases, diffusion through cytoplasm, or nuclear import. Complementary analysis of cellular uptake with consideration of the ζ potentials of the transfection particles (Table S1) was poorly informative as well, but confirmed that protein coronas formed around the lipoplexes even at low serum concentration (10%), masking their net negative charge and conditioning their interaction with the cell membrane and subsequent internalization.

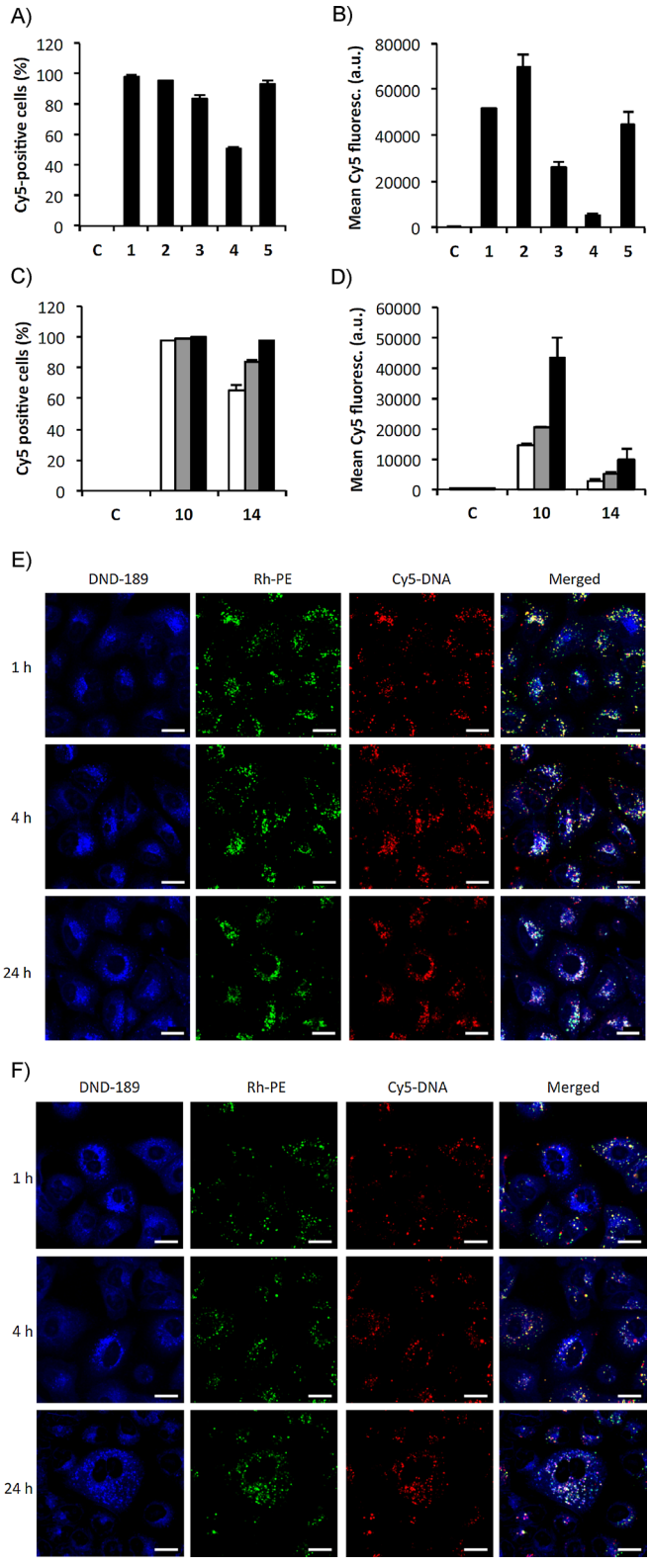

Figure 2. A) Cellular uptake of lipoplexes in BHK-21 cells, and B) mean fluorescence of cells quantified by flow cytometry analysis (λ_{ex} = 640 nm, analysis at 660 nm). Lipoplexes were prepared at N/P = 1 from Cy5-labeled DNA and lipids **1**–**5**, and were incubated for 4 h before treatment and analysis. Values for each sample are the means of duplicate determination. "**C**" (control) refers to untreated cells. C), D) Time courses of cellular uptake. Lipoplexes were prepared with lipids **1** and **4** and Cy5-DNA (N/P = 1). C) The populations of Cy5-positive cells, and D) the mean fluorescence intensities of cells were measured at 1 (white), 2 (gray), and 4 h (black) after the cells had been treated with lipoplexes. E), F) Confocal microscopy images of the intracellular trafficking of DNA complexes prepared with conjugates E) **1**, and F) **4**. Lipoplexes were prepared with Cy5-labeled DNA and the corresponding conjugate (N/P = 1) with 1% molar Rh-PE, and incubated with A549 cells. Prior to observation 1, 4, and 24 h after addition of lipoplexes, cells were stained with LysoSensor green DND-189 to indicate acidic organelles (scale bar: 20 μm).

The cellular uptake of the DNA complexes was kinetically investigated, and analysis was especially focused on DNA complexes with conjugate **1** and its analogue **4** with improved biodegradability (Figure 2C, D). Flow cytometry analysis was performed 1, 2, and 4 h after cell incubation with the lipoplexes had started. As might be expected, the intensity of Cy5 fluorescence increased almost linearly during the incubation period. However, a significant difference was observed when the internalization rates were considered. Indeed, cellular uptake of **1**·DNA complexes proceeded four to five times more quickly than that of **4**·DNA particles, which was consistent with the transfection data obtained after 24 h incubation time (Figure 1A). This suggested that, once inside cells, the two transfection particles released functional DNA at similar rates.

To gain insight into the intracellular distribution and disaggregation of the transfection particles, A549 cells were incubated with double-labeled lipoplexes ($N/P = 1$) incorporating Rh-PE and Cy5-labeled DNA. Cells were imaged at different time points by confocal microscopy.

Lipoplexes prepared with conjugate **1** were massively internalized in cells, appearing as punctate green (Rh channel) or red (Cy5 channel) structures (Figure 2E). Quantitative image analysis by conventional pixel counting methods[28] indicated that only 4% of rhodamine-labeled particles collocated with acidic organelles after incubation for 1 h (Table S3). Collocation had increased to 21 and 57% after 4 and 24 h, respectively. The same was observed when the cyanine dye channel was considered (5, 17, and 68% collocation was measured after 1, 4, and 24 h, respectively). These data were consistent with a decrease in the intracellular processing rate of the lipoplexes along the incubation period, resulting in an accumulation of transfection particles inside cells. Similar observations have been reported previously.[29] Substantial location of rhodamine fluorescence (96, 79, and 43% after 1, 4, and 24 h, respectively) and Cy5 fluorescence (95, 83, and 32% after 1, 4, and 24 h, respectively) outside acidic intracellular compartments, however, indicated that a significant amount of lipoplexes had gained access to the cytosol.

DNA complexes prepared with conjugate **4** behaved differently (Figure 2F). Firstly, less fluorescent material was internalized by cells; this was consistent with the results obtained in the flow cytometry study. Secondly, accumulation of the lipoplexes in the endosomes over time was reduced by a factor of 2–3 relative to **1**·DNA lipoplexes. Indeed, whereas 68% of detectable DNA appeared enclosed in acidic compartments after 24 h with carrier **1**, this ratio dropped to 16% with carrier **4**. This was the indication that the major proportion of internalized DNA molecules (84%) had gained access to the cytosol. Thus, it can reasonably be proposed that improved endosome escape was the result of the higher biodegradability of conjugate **4** relative to **1**, the larger quantity of $C_{12}E_4$ produced inside the compartment being responsible for higher membrane permeabilization. Because conjugate hydrolysis was also expected to affect lipoplex stability, we made attempts to quantify intracellular complex disaggregation through FRET measurements. Because of a lack of sensitivity of our experimental setup that could not image Cy5-DNA at sub-micromolar concentrations, data analysis proved troublesome. Nevertheless, on considering the collocation of rhodamine and Cy5 fluorescence, a higher score was generally obtained with conjugate **4**. Fully condensed transfection particles could hardly be detected through the Rh channel due to FRET with the Cy5 acceptor (Figure S5), so this was an indication that **4**·DNA complexes were indeed more quickly disaggregated than **1**·DNA complexes inside cells.

In vitro gene silencing with the DOPC–detergent conjugate/siRNA complexes

Some previously described phospholipid–detergent conjugates have been demonstrated to be efficient carriers for intracellular delivery of siRNA.[14–15] We thus examined the ability of conjugate **1** to deliver siRNA into cultured cells (Figure 3, left). We used the A549-Luc cell line, which has been stably transformed to express a luciferase gene. Transfection particles were prepared with a specific luciferase-targeting siRNA (siLuc), and gene knockdown was determined 48 h after contact with the cells. Non-targeting siRNA (sic) was used as a control to provide crucial information on the toxicity induced by the lipoplexes. We investigated in vitro efficacy at low doses of both conjugate **1** and siRNA in the meantime. The dose/response study showed that conjugate **1** was able to promote silencing of the luciferase gene in cultured cells up to 95% at low siRNA and lipid concentrations (5–10 nM and at 5.5 μM, respectively). When the amount of siRNA delivered to the cells was reduced by a factor of two (2.5 nM; that is, 7 ng siRNA per well) approximately 80% silencing could still be achieved. Furthermore, no significant LDH release was measured at the lower lipid concentration, although gene silencing was extremely effective (Figure 3, right). Increasing the amount of lipid delivered to the cells led to a synchronous increase in LDH release, and at high lipid concentration (22 μM) marked cytotoxicity was ob-

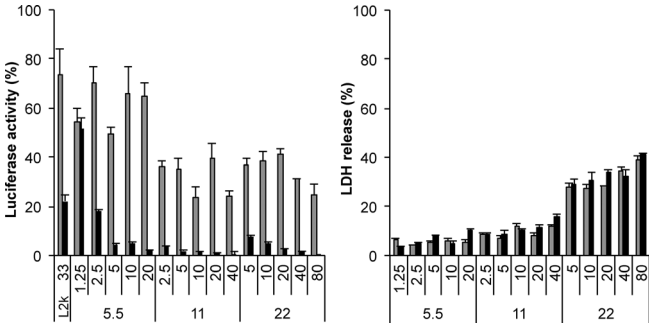

Figure 3. Efficiency of **1** in delivering siRNA in A549-Luc cells at various lipid and siRNA concentrations (left), together with associated cytotoxicity (right). For comparison, Lipofectamine 2000 was assayed in parallel according to the optimized experimental conditions provided by the supplier (33 nM siRNA). Conjugate **1** (5.5, 11, 22 μM, second line abscissa axis) was formulated either with non-targeting siRNA (sic: gray) or with luciferase-targeting siRNA (siLuc: black) at various concentrations (1.25 to 80 nM, first line abscissa axis) and added to the cells according to a reverse transfection procedure as indicated in the Experimental Section.

served. Moreover, it is worth noting that conjugate **1** was more potent than the commercially available transfection reagent Lipofectamine 2000 (L2k). The latter was assayed according to the optimized experimental conditions provided by the supplier (33 nM siRNA) and led to 78% gene knockdown. Similar activity (82% knockdown) was achieved with conjugate **1** at lower siRNA concentration (2.5 nM), and silencing was improved to 96% when the siRNA concentration was increased to 5 nM.

Because of the activity profile of the labile analogues of lipid–detergent conjugate **1** in DNA delivery (vide supra), there was great interest in determining the efficiency of conjugates **2**–**5** in delivering siRNA. This work was carried out with A549-Luc cells over an extended range of siRNA and carrier concentrations, by determining the luciferase gene knockdown (Figure 4) and the cytotoxicity (Figure S4) induced by the resulting formulations. The labile conjugates **2**, **3**, and **5** displayed knockdown efficiencies (90–95%) similar to that obtained with the parent compound **1**. This, however, required the use of a larger amount of carriers (12 μM), possibly to compensate for their premature or accelerated hydrolysis. Furthermore, as already observed with DNA, the particles resulting from the complexation of siRNA by conjugates **1**–**5** displayed very similar sizes and ζ potentials (Table S2). This presumably allows more confident connection between the transfection efficiencies and the intracellular degradation rates of these conjugates.

With respect to the cytotoxicity of the formulations, compound **5** appeared to be better tolerated by the cells, followed by **3**, and then **2**, although the differences were not very pronounced. In addition, cationic lipid **4**, bearing an isopropyl substituent on the acetal bridge, failed to provoke specific luciferase silencing over the whole concentration range tested. In this case, important luciferase silencing was achieved regardless of the siRNA used (i.e., either targeting or control siRNA), suggesting toxicity concerns that were indeed supported by the LDH release data (Figure S4). Parallel to the findings from the previous DNA delivery experiments, it turned out that improving biodegradability of the cationic conjugates did not improve in vitro siRNA delivery efficiency. Although high transfection rates could be obtained, this usually required larger amounts of carrier and came with significant associated toxicity.

In vivo transfection efficiency and inflammatory effect of the DOPC–detergent conjugate·DNA complexes

Our ongoing research goals are mainly focused on therapeutic gene delivery by the pulmonary route to treat disorders such as cystic fibrosis (CF), chronic obstructive pulmonary diseases (COPDs), and asthma, which are among the more representative causes of mortality and morbidity worldwide.[30] In this context, a gene therapy approach based on local delivery of nucleic acid to the lung might be especially advantageous because it reduces systemic side effects and does not lead to interactions between lipoplexes and serum proteins en route. Thus, in order to determine whether findings from the in vitro experiments presented above could translate into gene delivery efficiency in vivo, DNA formulations based on conjugates **1** and **2** were evaluated in mice through the airway route. Because PEGylation of cationic lipid-based carriers has been shown to be crucial for providing lipoplexes with the necessary extended lifetime in the animal body,[31] we introduced DMPE-mPEG$_{5000}$ into the formulations, as well as DOPE, a frequently used lipid helper. The resulting transfection particles were administered to mice by intranasal instillation, and luciferase expression and inflammatory response were measured in the lung tissue at 24 h post-administration.

Preliminary in vitro evaluation of these formulations was not very informative because PEGylation of lipoplexes is known to be detrimental to transfection efficiency in cultured cells (Figure S6A).[32] This is the result of steric shielding by PEG that not only reduces undesired interactions of transfection particles with components of the cell culture medium, but also sup-

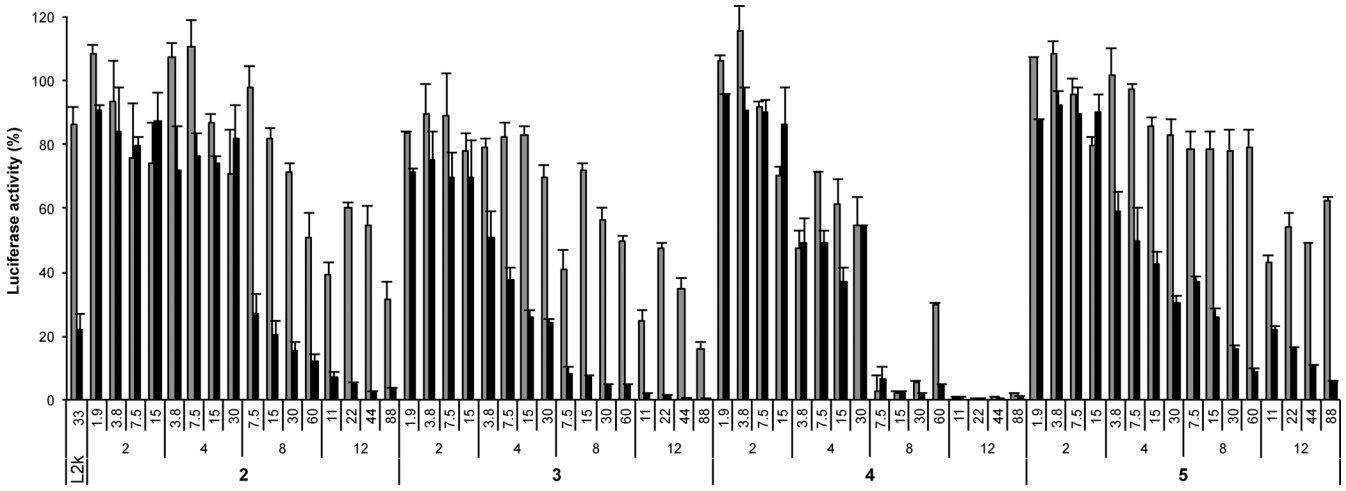

Figure 4. Efficiency of **2**–**5** and of Lipofectamine 2000 in delivering siRNA in luciferase-expressing A549-Luc cells. The culture medium contained 10% FBS. Conjugates (2, 4, 8, 12 μM, second line abscissa axis) were formulated either with non-targeting siRNA (sic: gray) or with luciferase-targeting siRNA (siLuc: black) at various concentrations (1.9 to 88 nM, first line abscissa axis). Luciferase activity was measured after a 48 h incubation period.

presses the electrostatic interactions with the plasma and endosome membranes that are conducive to cellular uptake and endosome escape, respectively. With regard to the DOPE component, although it failed to improve the transfection rate by the DOPC–detergent conjugates in vitro (Figure S6B), it proved to be necessary for eliciting significant transfection activity in vivo (Figure 5). Indeed, formulation B (**1**/DOPE/DMPE-mPEG$_{5000}$

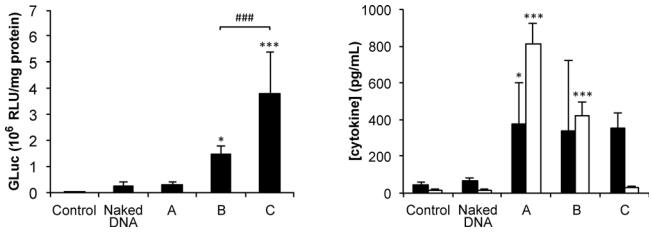

Figure 5. In vivo transfection efficiencies (left) and inflammatory responses [right, IL-6 (black bars), KC (white bars)] of formulations based on conjugate **1** and its biolabile analogue **2** (A: **1**/DMPE-mPEG$_{5000}$ 1:0.05; B: **1**/DOPE/DMPE-mPEG$_{5000}$ 1:1:0.05; C: **2**/DOPE/DMPE-mPEG$_{5000}$ 1:1:0.02). DNA (pCMV-GLuc, 40 μg) was administered as a single dose in pure water (50 μL). Animals were euthanized 24 h post-administration for determination of luciferase expression in lung homogenate ($n=4$). Control and naked DNA refer to mice that received either pure water (50 μL) or DNA (40 μg) in pure water (50 μL), without carrier. Statistically significant differences at $^*p<0.05$ and $^{***}p<0.001$ relative to naked DNA (left) or control (right) as determined by a one way ANOVA followed by the Dunnett multiple comparison test.

1:1:0.05, mol%) improved luciferase expression in the mouse lung by a factor of 5 (1.45×10^6 versus 0.29×10^6 RLU per mg protein) relative to the DOPE-free formulation A. On the other hand, although it did not prove superior to **1** in vitro, biolabile conjugate **2** proved much more potent in vivo (formulation C, **2**/DOPE/DMPE-mPEG$_{5000}$ 1:1:0.02), with transfection efficiency being improved by an additional factor of 2.6 (3.78×10^6 RLU per mg protein).

Moreover, on consideration of the inflammatory response that characterizes cationic-lipid-mediated gene transfer, interesting results were obtained as well. The levels of two cytokines involved in acute inflammation—interleukin-6 (IL-6) and keratinocyte-derived chemokine (KC)—were measured in bronchoalveolar lavage fluids (BALFs) of treated mice. These cytokines are secreted by polymorphonuclear neutrophils (PMNs) and are critical in the unfolding of the inflammatory response and in establishing the correct environmental conditions for launch of the adaptive immune response.[33] IL-6 production was found to be stable for the three formulations investigated (<380 pg per mL BALF) and did not increase with transfection efficiency. More strikingly, KC secretion, established at (814 ± 112) and (423 ± 76) pg mL^{-1} with formulations A and B, respectively, dropped to (29.4 ± 9.3) pg mL^{-1} with formulation C: that is, the one containing the biolabile conjugate **2**. Such a value was not significantly different from that measured for the negative controls [(15.7 ± 8.8) pg mL^{-1}]. Although these preliminary results deserve additional investigation, they suggest that conjugate **2** might be a promising DNA carrier for pulmonary delivery.

Conclusion

Phospholipid–detergent conjugates have previously been reported as valuable tools for in vitro DNA and siRNA delivery. The work described here aimed to improve the transfection efficiencies and intrinsic toxicity profiles of these nucleic acid carriers so that they might be transformed into candidates for in vivo gene transfer applications. Our working hypothesis implies a Trojan horse mechanism. The efficiency of the conjugates designed in this study is based on the membrane-disrupting properties of the detergent molecule produced through the biodegradation of the carrier within the endosome acidic compartment. The results obtained show that conjugation of DOPC with $C_{12}E_4$ can produce versatile carriers that can deliver DNA both in vitro and in vivo, with high efficiency and low toxicity. On the one hand, structure–activity relationships within the conjugate series suggest that compound **1** might represent a reasonable compromise between 1) the membrane activity of the detergent released in situ, and 2) the susceptibility of the conjugate to degradation enzymes.

Improving degradability of the conjugates did not lead to higher gene delivery efficiency in vitro. Rather, to maintain a high transfection rate, larger amounts of the more labile conjugates were required, with subsequent higher associated cytotoxicity. A conclusion might be that the rate of in vitro degradation of the phosphotriester group in the conjugates is not a limiting step for suitable expression of the transgene in cultured cells. In contrast, siRNA delivery proved to be more sensitive to the carrier stability. Although significant transfection efficiency could be attained with conjugates displaying enhanced biodegradability, this required larger amounts of carrier with respect to the siRNA cargo, and came along with marked toxicity. A limit was reached with the most labile carrier in the series, the gene silencing efficiency of which, if any, was fully masked by cytotoxicity.

Finally, the previous findings did translate into gene delivery efficiency in vivo, and high transgene expression was obtained in the mouse lung with a biodegradable analogue of DOPC–detergent conjugate **1**. Besides improving in vivo transfection efficiency, biodegradability of the conjugate allowed significant reduction of the inflammatory response that characterizes cationic-lipid-mediated gene transfer in animals. Thus, biodegradable DOPC–detergent conjugates might represent promising DNA carriers for pulmonary delivery.

Experimental Section

Materials: Unless otherwise stated, all chemical reagents were purchased from Alfa Aesar (Bischeim, France) and were used as received. DOPC was from Lipoid GmbH (Germany). When required, solvents were dried by standard procedures just before use.[34] TLC was performed with precoated plates (0.25 mm Silica Gel 60 F_{254}, Merck, Darmstadt, Germany). Products were purified by chromatography over silica gel (Silica Gel 60, 40–63 μm, Merck). NMR spectra were recorded with Bruker 300 MHz Avance DPX and 400 MHz Avance III instruments. ^{1}H, ^{13}C, and ^{31}P NMR chemical shifts (δ) are reported in ppm relative to their standard reference (^{1}H: $CHCl_3$ at 7.27 ppm; ^{13}C: $CDCl_3$ at 77.0 ppm; ^{31}P: H_3PO_4 at 0.00 ppm). IR spec-

tra were recorded with a FTIR Nicolet 380 spectrometer in the ATR mode, and absorption values (ν) are in wave numbers [cm^{-1}]. Mass spectra were recorded with an Agilent technology 6520 Accurate Mass QToF instrument in electrospray ionization (ESI) mode. Mass data are reported in mass units (*m/z*). Lipofectamine 2000 and LysoSensor green DND-189 were obtained from Invitrogen (Cergy Pontoise, France). 1,2-Dioleoyl-*sn*-glycero-3-phosphocholine (DOPC), 1,2-dioleoyl-*sn*-glycero-3-phospho-ethanolamine (DOPE), 1,2-dioleoyl-*sn*-glycero-3-phosphoglycerol (DOPG), 1,2-dimyristoyl-*sn*-glycero-3-phosphoethanolamine-*N*-[methoxy(polyethylene glycol)-5000] ammonium salt (DMPE-$mPEG_{5000}$), 1,2-dioleoyl-*sn*-glycero-3-phospho-ethanolamine-*N*-(7-nitro-2–1,3-benzoxadiazol-4-yl ammonium salt (NBD-PE), and 1,2-dioleoyl-*sn*-glycero-3-phosphoethanolamine-*N*-(lissamine rhodamine B sulfonyl) (Rh-PE) were from Avanti Polar Lipids. Cholesterol (chol) was from Sigma–Aldrich. BHK-21 cells (Syrian hamster kidney cells, CCL-10), Calu-3 cells (epithelial lung adenocarcinoma, HBT-55), A549 cells (human lung carcinoma, CCL-185), and NCI-H292 cells (human lung mucoepidermoid carcinoma, CRL-1848) were obtained from ATCC-LGC (Molsheim, France). pCMV-FLuc expression plasmid (5.5 kbp, BD Biosciences Clontech, Franklin Lakes, NJ, USA) was used as reporter gene to monitor DNA transfection activity in vitro.[35] This plasmid encodes the firefly luciferase gene under the control of a strong CMV promoter. Plasmid pCMV-GLuc (5.7 kbp, Nanolight Technology, Pinetop, AZ, USA) was used as reporter gene to monitor in vivo DNA transfection activity.[36] This plasmid encodes the *Gaussia* luciferase gene under the control of the CMV promoter. The A549 cell line was transformed to allow stable expression of the *Photinus pyralis* luciferase gene originating from the pGL3 plasmid (Clontech, Mountain View, CA) to assess siRNA delivery.[37] The pGL3 plasmid also encoded for a gene conferring resistance to the antibiotic G418. This antibiotic was thus used to select the transfected A549-Luc cells. Luciferase-gene-silencing experiments were performed with an RNA duplex (siLuc) of the sense sequence: 5′-CUU ACG CUG AGU ACU UCG A. Control untargeted RNA duplex (sic) was of sense sequence: 5′-CGU ACG CGG AAU ACU UCG A. Both RNAs were from Eurogentec (Angers, France). DNA concentration refers to phosphate content. Culture media (Dulbecco's modified Eagle's medium, DMEM; Roswell Park Memorial Institute medium, RPMI 1640), FBS, and supplements were from GIBCO-BRL (Cergy-Pontoise, France). Lysis and luciferin solutions for monitoring Firefly luciferase activity were purchased from Promega. Coelenterazine substrate for monitoring *Gaussia* luciferase activity was from Nanolight Technology.

Conjugate 2: Chloromethyl chloroformate (522 μL, 5.94 mmol) was added to a solution of **7** (2.00 g, 5.40 mmol) and pyridine (547 μL, 6.79 mmol) in freshly distilled CH_2Cl_2 (40 mL). The reaction mixture was stirred at rt under argon for 18 h, neutralized with water (50 mL), and extracted with EtOAc. The organic layer was dried over Na_2SO_4 and filtered, and volatiles were removed under reduced pressure. Compound **9** was obtained as a colorless oil (2.26 g, 92%) and was used in the next step without further purification. TLC R_f = 0.60 (CH_2Cl_2/MeOH 90:10); ^{1}H NMR (400 MHz, $CDCl_3$): δ = 5.68 (s, 2H), 4.33–4.30 (m, 2H), 3.70–3.68 (m, 2H), 3.60–3.57 (m, 16H), 3.53–3.50 (m, 2H), 1.52–1.50 (m, 2H), 1.26–1.20 (m, 18H), 0.82 ppm (t, $^3J_{H,H}$ = 6.6 Hz, 3H); ^{13}C NMR (100 MHz, $CDCl_3$): δ = 153.5, 72.3, 71.6, 70.8, 70.7, 70.1, 66.7, 32.0, 29.8, 29.6, 26.2, 22.7, 14.2 ppm; FTIR (film): $\tilde{\nu}$ = 2922, 2854, 2360, 2341, 1766, 1250, 1108 cm^{-1}.

A solution of compound **9** (1.95 g, 4.28 mmol) in dry $CHCl_3$ (5 mL) was added to a solution of DOPC (421 mg, 0.54 mmol) in freshly distilled $CHCl_3$ (10 mL). The resulting reaction mixture was heated at reflux for 20 h under argon and then cooled down and concentrated under reduced pressure at 20 °C. The crude residue was purified by flash chromatography over silica gel (CH_2Cl_2/MeOH 88:12 to 80:20) to yield compound **2** as a waxy solid (130 mg, 20%, two diastereomers, ammonium chloride). TLC R_f = 0.53 (CH_2Cl_2/MeOH 90:10); ^{1}H NMR (400 MHz, $CDCl_3$): δ = 5.69–5.59 (m, 2H), 5.35–5.25 (m, 4H), 5.24–5.17 (m, 1H), 5.63–5.61 (br m, 2H), 4.39–4.06 (m, 8H), 3.71 (t, $^3J_{H,H}$ = 4.7 Hz, 2H), 3.65–3.50 (m, 18H), 3.46 (s, 9H), 3.40 (t, $^3J_{H,H}$ = 6.9 Hz, 2H), 2.36–2.40 (m, 4H), 2.05–1.90 (m, 8H), 1.65–1.47 (m, 2H), 1.36–1.15 (m, 58H), 1.05 (t, $^3J_{H,H}$ = 6.6 Hz, 6H), 0.84 ppm (t, J = 6.7 Hz, 9H); ^{13}C NMR (100 MHz, $CDCl_3$): δ = 173.4, 173.0, 153.5, 130.2, 129.9, 86.2, 71.7, 70.7, 70.2, 69.4, 68.7, 68.2, 66.8, 66.7, 65.5, 65.4, 62.4, 61.6, 54.7, 34.2, 32.1, 29.9, 29.8, 29.7, 29.6, 29.5, 29.4, 29.3, 29.2, 27.4, 27.3, 26.2, 25.1, 22.9, 14.2 ppm; ^{31}P NMR (162 MHz, $CDCl_3$): δ = −3.2, −3.3 ppm; FTIR (film): $\tilde{\nu}$ = 2922, 2852, 2360, 2341, 1741, 1260 cm^{-1}; MS (ESI): *m/z* calcd for $C_{58}H_{111}NO_{11}P(C_2H_4O)_4^+$: 1204.89 $[M-Cl]^+$; found: 1204.8.

Conjugate 3: Intermediate 1-chloroethyl carbonate **10** was prepared from **7** (2.00 g, 5.40 mmol) and chloroethyl chloroformate (641 μL, 5.94 mmol) by the same procedure as for **9**. It was obtained as a colorless oil (2.33 g, 92%) and was used in the next step without further purification. TLC R_f = 0.55 (CH_2Cl_2/MeOH 90:10); ^{1}H NMR (400 MHz, $CDCl_3$): δ = 6.4 (q, $^3J_{H,H}$ = 5.8 Hz, 1H), 4.34–4.32 (m, 2H), 3.72 (t $^3J_{H,H}$ = 4.1 Hz, 2H), 3.63–3.54 (m, 16H), 3.42 (t, $^3J_{H,H}$ = 6.8 Hz, 2H), 1.81 (d, $^3J_{H,H}$ = 5.8 Hz, 3H), 1.57–1.53 (m, 2H), 1.29–1.23 (m, 18H), 0.86 ppm (t, $^3J_{H,H}$ = 6.7 Hz, 3H); ^{13}C NMR (100 MHz, $CDCl_3$): δ = 153.1, 84.8, 71.8, 70.9, 70.8, 70.2, 68.9, 68.1, 32.1, 29.8, 29.7, 29.6, 26.3, 25.4, 22.9, 14.3 ppm.

Conjugate **3** was obtained as a waxy solid (290 mg, 37%, four diastereomers, ammonium chloride) from **10** (2.33 g, 4.96 mmol) and DOPC (488 mg, 0.62 mmol) by the same procedure as for **2**. TLC R_f = 0.53 (CH_2Cl_2/MeOH 90:10); ^{1}H NMR (400 MHz, $CDCl_3$): δ = 6.41–6.21 (m, 1H), 5.37–5.24 (m, 4H), 5.24–5.17 (m, 1H), 4.54 (br m, 2H), 4.38–4.05 (m, 8H), 3.83–3.86 (m, 2H), 3.65–3.50 (m, 18H), 3.46 (s, 9H), 3.40 (t, $^3J_{H,H}$ = 6.9 Hz, 2H), 2.36–2.23 (m, 4H), 2.05–1.90 (m, 8H), 1.65–1.47 (m, 9H), 1.36–1.15 (m, 58H), 0.84 ppm (t, $^3J_{H,H}$ = 6.7 Hz, 9H); ^{13}C NMR (100 MHz, $CDCl_3$): δ = 173.4, 173.0, 153.1, 95.7, 95.3, 71.1, 70.8, 70.7, 70.2, 69.6, 69.5, 69.3, 69.2, 68.8, 68.1, 66.8, 68.1, 66.8, 66.7, 66.6, 66.4, 66.3, 66.2, 65.5, 65.4, 62.5, 62.2, 61.7, 61.6, 61.5, 54.6, 34.3, 34.2, 32.1, 30.4, 29.9, 29.6, 29.4, 29.3, 27.4, 26.3, 25.2, 25.0, 23.7, 22.9, 21.4, 20.9, 14.3 ppm; ^{31}P NMR (162 MHz, $CDCl_3$): δ = −5.3, −5.5, −5.7, −5.9 ppm; FTIR (film): $\tilde{\nu}$ = 2922, 2852, 1743, 1457, 1264, 1108, 1084, 971, 669 cm^{-1}; MS (ESI): *m/z* calcd for $C_{59}H_{113}NO_{11}P(C_2H_4O)_4^+$: 1218.91 $[M-Cl]^+$; found: 1218.9.

Conjugate 4: Intermediate 1-chloro-2-methylpropyl carbonate **11** (2.58 g, 96%) was prepared from **7** (2.00 g, 5.40 mmol) and 1-chloro-2-methylpropyl chloroformate (884 μL, 5.94 mmol) by the same procedure as for **9**. It was obtained as a colorless oil (2.58 g, 96%) and was used in the next step without further purification. TLC R_f 0.50 (CH_2Cl_2/MeOH 90:10); ^{1}H NMR (400 MHz, $CDCl_3$): δ = 6.16 (d, $^3J_{H,H}$ = 4.5 Hz, 1H), 4.34–4.32 (m, 2H), 3.73 (t, $^3J_{H,H}$ = 4.5 Hz, 2H), 3.64–3.54 (m, 16H), 3.42 (t, $^3J_{H,H}$ = 6.8 Hz, 2H), 2.23–2.16 (m, 1H), 1.63–1.48 (m, 2H), 1.29–1.23 (m, 18H), 1.05 (t, $^3J_{H,H}$ = 6.6 Hz, 6H), 0.86 ppm (t, $^3J_{H,H}$ = 6.7 Hz); ^{13}C NMR (100 MHz, $CDCl_3$): δ = 92.8, 71.6, 70.7, 70.6 (4C), 70.1, 68.7, 67.8, 35.2, 31.9, 29.6 (4C), 29.5, 29.3, 26.1, 22.7, 17.4, 17.1, 14.1 ppm.

Conjugate **4** was obtained as a waxy solid (174 mg, 20%, four diastereomers, ammonium chloride) from **11** (2.70 g, 5.43 mmol) and DOPC (533 mg, 0.68 mmol) by the same procedure as for **2**. TLC R_f = 0.53 (CH_2Cl_2/MeOH 90:10). ^{1}H NMR (400 MHz, $CDCl_3$): δ = 6.16–6.10 (m, 1H), 5.35–5.20 (m, 5H), 4.57 (br m, 2H), 4.47–4.12 (m, 8H),

3.84–3.72 (m, 2H), 3.70–3.65 (m, 18H), 3.46 (t, $^3J_{H,H}=6.1$ Hz, 2H), 3.25 (s, 9H), 2.40–2.29 (m, 4H), 2.18–2.07 (m, 1H), 2.06–1.95 (m, 8H), 1.69–1.50 (m, 6H), 1.39–1.22 (m, 58H), 1.08–0.99 (m, 6H), 0.88 ppm (t, $^3J_{H,H}=6.7$ Hz, 9H); ^{13}C NMR (100 MHz, $CDCl_3$): $\delta=$ 174.7, 154.7, 130.9, 130.6, 101.7, 101.6, 78.5, 72.4, 71.4, 71.3, 71.0, 70.7, 70.6, 69.7, 69.6, 68.9, 67.6, 66.7, 66.6, 54.8, 35.0, 34.9, 33.9, 32.9, 30.9, 30.6, 30.4, 30.2, 30.1, 28.1, 27.1, 25.9, 23.6, 18.4, 16.8, 16.7, 16.4, 14.6 ppm; ^{31}P NMR (162 MHz, $CDCl_3$): $\delta=-4.7$, -4.8, -4.9, -5.1 ppm; FTIR (film): $\tilde{\nu}=2925$, 2854, 1745, 1510, 1258, 1160, 1092, 1031, 637 cm^{-1}; MS (ESI): *m/z* calcd for $C_{61}H_{117}NO_{11}P(C_2H_4O)_4^+$: 1246.94 $[M-Cl]^+$; found: 1246.9.

Conjugate 5: A mixture of compound **7** (4.00 g, 10.86 mmol) and succinic anhydride (3.26 g, 32.6 mmol) in dry pyridine (30 mL) was stirred at room temperature for 18 h. Volatiles were removed under reduced pressure, and the crude residue was stirred in aqueous $NaHCO_3$ (5%) for 30 min, acidified to pH 3 with HCl (12 N), and extracted with CH_2Cl_2/MeOH (2:1, *v/v*). The combined organic layers were dried over Na_2SO_4, filtered, and concentrated under reduced pressure. The crude residue was purified by flash chromatography over silica gel (CH_2Cl_2/MeOH 95:5) to yield the intermediate hemisuccinate derivative **12** as a waxy solid (4.76 g, 95%). TLC $R_f=0.46$ (CH_2Cl_2/MeOH 90:10); ^{1}H NMR (400 MHz, $CDCl_3$): $\delta=4.25$–4.23 (m, 2H), 3.67–3.40 (m, 16H), 3.44–3.40 (t, $^3J_{H,H}=8.8$ Hz, 2H), 2.63 (m, 2H), 1.56–1.53 (m, 2H), 1.27–1.23 (m, 18H), 0.85 ppm (t, $^3J_{H,H}=6.5$ Hz, 3H); ^{13}C NMR (100 MHz, $CDCl_3$): $\delta=175.9$, 172.2, 71.6, 70.7, 70.6, 70.1, 69.1, 63.9, 32.0, 29.7, 29.6, 29.3, 29.2, 29.0, 26.2, 22.7, 14.2 ppm; FTIR (film): $\tilde{\nu}=2923$, 2853, 1735, 1457, 1249, 1113, 669 cm^{-1}.

nBu$_4$NHSO$_4$ (284 mg, 0.87 mmol) and Na_2CO_3 (1.83 g, 17.30 mmol) were added to a suspension of the previous ester (2.00 g, 4.33 mmol) in water (40 mL), and the reaction mixture was stirred for 20 min at rt, affording a clear solution. The mixture was then cooled down to 0 °C, and a solution of chloromethyl chlorosulfate (569 μL, 5.62 mmol) in dry CH_2Cl_2 (40 mL) was added dropwise over 5 min. The resulting white suspension was vigorously stirred for 1 h at 0 °C and for 18 h at room temperature. The organic layer was separated, and the aqueous phase was extracted with CH_2Cl_2. The combined organic layers were dried over Na_2SO_4, filtered, and concentrated under reduced pressure. Compound **13** was obtained as a yellow oil (2.19 g, 99%) and was used in the next step without further purification. TLC $R_f=0.47$ (CH_2Cl_2/MeOH 90:10); ^{1}H NMR (400 MHz, $CDCl_3$): $\delta=5.68$ (s, 2H), 4.24–4.21 (m, 2H), 3.68–3.59 (m, 16H), 3.41 (t, $^3J_{H,H}=6.8$ Hz, 2H), 2.68 (s, 2H), 1.57–1.50 (m, 2H), 1.32–1.16 (m, 18H), 0.85 ppm (t, $^3J_{H,H}=6.8$ Hz, 3H); ^{13}C NMR (100 MHz, $CDCl_3$): $\delta=171.9$, 170.6, 71.7, 70.8 (2C), 69.2, 68.9, 64.2, 32.1, 29.9, 29.8 (2C), 29.7, 29.6, 29.1, 28.9, 26.3, 22.8, 14.3 ppm.

Conjugate **5** was obtained as a waxy solid (147 mg, 21%, two diastereomers, ammonium chloride) from **13** (2.19 g, 4.28 mmol) and DOPC (423 mg, 0.54 mmol) by the same procedure as for **2**. TLC $R_f=0.16$ (CH_2Cl_2/MeOH 90:10); ^{1}H NMR (400 MHz, $CDCl_3$): $\delta=5.74$–5.61 (m, 2H), 5.37–5.26 (m, 5H), 4.56 (br m, 2H), 4.44–4.12 (m, 8H), 3.85–3.75 (m, 2H), 3.65–3.53 (m, 18H), 3.4 (t, $^3J_{H,H}=6.9$ Hz, 2H), 3.25 (s, 9H), 2.77–2.65 (m, 4H), 2.40–2.28 (m, 4H), 2.05–1.95 (m, 8H), 1.67–1.5 (m, 6H), 1.39–1.22 (m, 58H), 0.86 ppm (t, $^3J_{H,H}=$ 6.7 Hz, 9H); ^{13}C NMR (100 MHz, $CDCl_3$): $\delta=173.5$, 173.1, 171.2, 130.3, 129.9, 83.2, 71.8, 70.8, 70.7, 70.2, 69.5, 69.1, 66.8, 66.6, 65.5, 64.4, 62.4, 61.7, 61.6, 54.8, 34.4, 34.2, 32.1, 29.9, 29.8, 29.7, 29.5, 29.4, 29.3, 28.9, 28.6, 27.4, 25.1, 22.9, 14.3 ppm; ^{31}P NMR (162 MHz, $CDCl_3$): $\delta=-3.4$, -3.6 ppm; FTIR (film): $\tilde{\nu}=2927$, 2842, 1732, 1440, 1109, 969 cm^{-1}. MS (ESI): *m/z* calcd for $C_{61}H_{115}NO_{12}P(C_2H_4O)_4^+$: 1260.92 $[M-Cl]^+$; found: 1260.9.

Animals: Nine-week-old male BALB/c mice were purchased from Charles River Laboratories (Saint-Germain-sur-l'Arbresle, France). They were housed in polycarbonate exhaust ventilated cages (M.I.C.E. cages, Animal Care Systems) at four mice per cage, with bedding made from spruce wood chips (Safe, Villemoisson, France). Ventilation in the cages was set to 10–12 changes per hour, according to the manufacturer's recommendations. The animal room was maintained under controlled environmental conditions, with a temperature of (20±2) °C, a relative humidity of (50±10)% and a 12 h/12 h light/dark cycle. Food (standard diet 4RF21, Mucedola) and tap water were available ad libitum. The animals were acclimated for 1 week before the initiation of the study. Animal experimentation was conducted with the approval of the government body that regulates animal research in France (Agreement number: AL/23/30/02/13).

DNA fluorescence labeling: Cy5-labeled DNA (Cy5-pCMV-GLuc) was prepared by use of the Label IT Cy5 Nucleic Acid Labeling Kit (Mirus, Madison, WI, USA), according to the manufacturer's instructions. The labeling density was determined by absorbance measurements at 1 Cy5 molecule/34 bp DNA.

Preparation of liposomes: For the hydrolysis rate measurements involving ^{31}P NMR spectroscopy, liposomes were prepared by a solvent injection technique.[20] Briefly, a dry lipid film (10 μmol) was dissolved in *i*PrOH (200 μL) and then injected by syringe (flow rate 600 μL min^{-1}) with stirring (stirring speed 400 rpm) into the appropriate aqueous buffer medium [800 μL, HEPES (10 mM, pH 7.4) or AcOK/AcOH (10 mM, pH 4.5)] at 22 °C.

Preparation of lipoplexes for in vitro testing: Typically, the appropriate volume of a freshly prepared solution of cationic lipid (2 mM in EtOH) was deposited at the bottom of a 500 μL polyethylene tube and dried under vacuum. Then, pCMV-FLuc DNA (40 μL at the required concentration in 4.5% glucose) or siRNA (siLuc or sic, 40 μL at the required concentration in 4.5% glucose) was added to the resulting lipid film. After stirring by vortex for 30 s, the preparation was allowed to stand at room temperature for 30 min before use.

Preparation of lipoplexes for in vivo testing: Typically, components of the desired formulation were first mixed at the appropriate molar ratio in $CHCl_3$/MeOH (2:1, *v/v*) in a glass sample vial. The solvent was removed under vacuum for at least 3 h. The dried lipid film was then hydrated for 10 min in pure water and vigorously vortexed for 2 min to generate liposomes. Lipid/DNA complexes were prepared by gently mixing equal volumes of liposomes and DNA. The complexes were allowed to form for 15 min at room temperature without handling. Finally, the mixture was homogenized by pipetting up and down and subsequently used for in vivo gene delivery experiments,

DLS measurements: The average particle sizes and ζ potentials of lipoplexes were measured with a Zetasizer nanoZS apparatus (Malvern Instruments, Paris, France). All measurements were performed with freshly prepared lipoplexes (vide supra) at 25 °C and in triplicate. Data were analyzed by use of the multimodal number distribution software supplied with the instrument and expressed as means (±SDs).

Cell culture: All cell lines were grown in culture flasks at 37 °C in a CO_2 (5%) humidified chamber. BHK-21, A549, and Calu-3 cells were grown in DMEM-F12 medium, whereas NCI-H292 cells were grown in RPMI 1640. For all cell lines, these media were supplemented with FBS (10%), L-glutamine (2 mM), penicillin (100 units mL^{-1}), and streptomycin (100 μg mL^{-1}). For A549 and

Calu-3 cells, DMEM-F12 was also supplemented with HEPES (5 mM). For NCI-H292, RPMI 1640 was also supplemented with sodium pyruvate (1 mM) and HEPES (10 mM). Selection of A549-Luc cells was performed by adding G418 (0.8 mg mL^{-1}) to the culture medium. For experiments, cells were released from culture flasks with trypsin and transferred to adapted culture devices (see below).

In vitro DNA transfection experiments: Cells were seeded into 96-well plates (Becton-Dickinson) at a density of 6000 cells/well in serum (100 μL) containing culture medium. After 24 h, freshly prepared DNA lipoplexes (10 μL; that is, 0.2 μg DNA) were added to the wells, and cells were then allowed to grow in the incubator without further handling. Luciferase gene expression was assessed 24 h after lipoplex addition by use of a commercial kit (Promega) with slight modifications to the manufacturer's recommendations as outlined below. Briefly, the cell culture medium was carefully removed. The adherent cells were washed with phosphate-buffered saline (PBS, 100 μL) and treated with the kit lysis buffer (20 μL) for 15 min. The samples were then diluted with PBS (150 μL), and luciferase content was measured by monitoring light production from a 5 μL aliquot sample for 1 s upon addition of the luciferin substrate (35 μL), with the aid of a luminometer (Berthold Centro LB960 XS, Thoiry, France). The value for each sample is the mean of a triplicate determination (±SD).

siRNA delivery experiments: Freshly prepared siRNA lipoplexes (40 μL, containing the appropriate siRNA quantity for a quadruplicate) were first diluted with serum-containing culture medium (360 μL) and then deposited in triplicate (100 μL) into the wells of an empty culture plate. Subsequently, a suspension of freshly passaged A549-Luc cells (100 μL, 8000 cells) was added to the preplated transfection complexes. Cells were then allowed to adhere and grow in the incubator without further handling. Luciferase gene expression was assessed 48 h later as described above, except that the PBS volume added for the dilution step was different (200 μL). The content of luciferase protein in each sample was reported as the residual luciferase activity relative to untreated cells (100%). The value for each sample is the mean of a triplicate determination (±SD).

Airway gene delivery in mice: The lipoplexes [pCMV-GLuc (40 μg) in pure water (50 μL)] were administered as single doses into the lungs of mice by intranasal instillation. Instillations were carried out under light anesthesia with ketamine (50 mg kg^{-1}, Imalgen, Merial, Lyon, France) and xylazine (3.33 mg kg^{-1}, Rompun, Bayer, Puteaux, France) given intraperitoneally (i.p.). Control animals received instillation of the same volume of water. Animals were kept in a 60° inclined supine position until recovery from anesthesia to promote airway delivery of the solution through breathing. This procedure allowed correct and reproducible delivery of the lipoplexes all through the respiratory tract up to the alveolar spaces, as was checked by using a dye. The experiment was terminated at 24 h (unless otherwise stated) by i.p. injection of an overdose of ketamine and xylazine. The trachea was cannulated to perform bronchoalveolar lavages. Lungs were washed by two instillations of ice-cold saline (0.5 mL) supplemented with EDTA (saline-EDTA, 2.6 mM). Bronchoalveolar lavage fluids (BALFs) were centrifuged (200 *g*, 5 min, 4 °C), and the resulting supernatant was stored at −20 °C until cytokine measurements. After thoracotomy, lungs were perfused in situ through the pulmonary artery with ice-cold PBS (10 mL), collected, frozen in liquid nitrogen, and stored at −80 °C until assessment of the *Gaussia* luciferase gene expression.

Lactate dehydrogenase assay: Measurement of LDH cell release was used to assess the cytotoxicity of the formulations. Typically, at the end of each transfection experiment, an aliquot of culture supernatant was transferred into a 96-well assay plate, and LDH activity was measured by use of a commercial kit (Cytotoxicity Detection Kit Plus, Roche Applied Science) according to the manufacturer's instructions. LDH activity was expressed as the percentage of the maximum LDH activity measured after treatment of the cells with the kit lysis solution. The value for each sample is the mean of a triplicate determination (±SD). LDH release values of less than 10% were considered insignificant.

Fluorescence-activated cell sorter (FACS) assay: To determine the cellular uptake of lipoplexes, BHK-21 cells were seeded in 12-well culture plates at 65 000 cells/well in complete culture medium 24 h before use. The cells were treated with lipoplexes prepared at the charge ratio $N/P = 1$ and containing Cy5-labeled DNA (2.5 μg/well) and the cationic lipid of interest with molar Rh-PE (double-labeled lipoplexes, 1%). Cells were incubated in a CO_2 (5%) humidified chamber for 1, 2, or 4 h at 37 °C. After removal of the culture medium and washing with PBS, cells were detached from culture plates by using trypsin-EDTA in PBS (0.5%), pelleted by centrifugation (120 *g*, 5 min, 4 °C), suspended in culture medium (100 μL) containing FBS (1%), and placed on ice. Just before analysis, Amido Black (2.5 mg mL^{-1} in serum-free culture medium, 12.9 μL) was added to quench extracellular fluorescence due to residual lipoplexes associated to the plasma membrane. For each sample, 20 000 gated events were evaluated with a 16-color BD FACSAria II flow cytometer (Becton Dickinson, San Jose, CA). Rh-PE was excited at 561 nm, and emission was detected at 610 nm. If FRET was present, acceptor emission was additionally detected at 660 nm. Excitation at 561 nm and emitted fluorescence was spatially and temporarily separated from a second laser, which excited the acceptor at 640 nm. The emitted fluorescence was detected at 660 nm. Thus, it was possible to measure the donor signal (561/610 nm), the acceptor signal (640/660 nm), and the FRET signal (561/660 nm) simultaneously for each sample. Data acquisition was performed with BD FACS Diva Software (version 6.1.3) and data analysis with FlowJo software (version 8.8.7, FlowJo, LLC, Ashland, OR).

Cell imaging: For confocal laser scanning microscopy, A549 cells were plated into 8-well IbiTreat μ-slides (Biovalley, Nanterre, France) at a density of 30 000 cells/well in complete culture medium 24 h before use. Next, double-labeled lipoplexes (vide supra, $N/P = 1$, 30 μL) were added. Cells were incubated at 37 °C for 1, 4, or 24 h in a CO_2 (5%) humidified chamber. Then the culture medium was removed, and cells were washed with pre-warmed (37 °C) culture medium and stained with LysoSensor green DND-189 (500 nM in pre-warmed culture medium, 300 μL) for 30 min to label endosomal/lysosomal organelles. Before observation, the culture supernatant was replaced with fresh pre-warmed culture medium (300 μL), and Amido Black (2.5 mg mL^{-1} in serum-free culture medium, 35 μL) was added to quench extracellular fluorescence due to residual lipoplexes associated to the plasma membrane. The intracellular distribution of lipoplexes was observed by confocal microscopy with a Leica SP2 microscope equipped with a 63× oil immersion objective (NA = 1.2). DND-189, Rh, and Cy5 were excited with 488, 561, and 635 nm laser diodes, respectively. The emission bands were detected with a photomultiplier. The positions and the widths of the detection channels were adjusted for each dye (DND-189: 500–540 nm, Rh: 580–620 nm, Cy5: 650–720 nm). Images (1024×1024 pixels with a pixel size of 116 nm) were sequentially acquired at 400 Hz for each channel randomly in the plate. In order to determine the degree of collocation with all

the possible color combinations, individual spots were identified with the "Localization microscopy" plugin developed by N. Stuurman for μManager software.[38] In practice, a region of interest of 4×4 pixels (464×464 nm) was defined for each individual frame. Then, spatially separated point spread function signals emitted by diffraction-limited spots were detected by means of local maxima and fitted with a 2D Gaussian distribution. By using this approach, it was possible to obtain the positions of endosomes (DND-189), lipoplexes (Rh), and labeled DNA (Cy5) for each individual image. Next, the position list obtained for a specific channel was used to determine the presence or the absence of the two other colors. To avoid false positives, a threshold was used to filter out spots with fluorescence signals below twice the background level. By applying this method, it was possible to generate collocation trace (color 1 vs. color 2) from which the degree of collocation was obtained (Pearson's correlation coefficient). In addition, by removing from the analysis the color 1 particles that do not overlap with the color 2 particles and vice versa, it was possible to determine the percentage of particles displaying colors 1 and 2 and collocating with color 3. Finally, the fraction of lipoplexes exhibiting FRET was evaluated by imaging the sample with a 561 nm laser and recording the signal in the Cy5 channel.

Cytokine assays: IL-6 and KC were measured in BALFs by use of ELISA kits, according to the manufacturer's instructions (BD Biosciences, Le Pont de Claix, France).

Statistics: Data are presented as means ±SDs. Statistical differences between groups were determined by one-way analysis of variance (ANOVA) followed by the Tukey or the Dunnett multiple comparison test, with use of KaleidaGraph 4.5 software (Synergy Software, Reading, PA, USA). Data were considered significantly different when $p < 0.05$ (*).

Acknowledgement

The authors are grateful for financial support from SATT Conectus Alsace.

Keywords: airway administration · detergents · drug delivery · gene delivery · lipids

[1] a) C. Baum, J. Dullmann, Z. X. Li, B. Fehse, J. Meyer, D. A. Williams, C. von Kalle, *Blood* **2003**, *101*, 2099 – 2114; b) H. Sakurai, K. Kawabata, F. Sakurai, S. Nakagawa, H. Mizuguchi, *Int. J. Pharm.* **2008**, *354*, 9 – 15.

[2] D. V. Schaffer, J. T. Koerber, K. I. Lim, *Annu. Rev. Biomed. Eng.* **2008**, *10*, 169 – 194.

[3] D. Bouard, N. Alazard-Dany, F. L. Cosset, *Br. J. Pharmacol.* **2009**, *157*, 153 – 165.

[4] www.bionews.org.uk/page_204696.asp, **2012**.

[5] H. Yin, R. L. Kanasty, A. A. Eltoukhy, A. J. Vegas, J. R. Dorkin, D. G. Anderson, *Nat. Rev. Genet.* **2014**, *15*, 541 – 555.

[6] C. R. Safinya, K. K. Ewert, R. N. Majzoub, C. Leal, *New J. Chem.* **2014**, *38*, 5164 – 5172.

[7] a) M. B. Bally, P. Harvie, F. M. P. Wong, S. Kong, E. K. Wasan, D. L. Reimer, *Adv. Drug Delivery Rev.* **1999**, *38*, 291 – 315; b) Y. Duan, S. B. Zhang, B. Wang, B. L. Yang, D. F. Zhi, *Expert Opin. Drug Delivery* **2009**, *6*, 1351 – 1361; c) C. Tros de Ilarduya, Y. Sun, N. Duezguenes, *Eur. J. Pharm. Sci.* **2010**, *40*, 159 – 170.

[8] M. Ruponen, S. Ronkko, P. Honkakoski, J. Pelkonen, M. Tammi, A. Urtti, *J. Biol. Chem.* **2001**, *276*, 33875 – 33880.

[9] A. J. Lin, N. L. Slack, A. Ahmad, C. X. George, C. E. Samuel, C. R. Safinya, *Biophys. J.* **2003**, *84*, 3307 – 3316.

[10] H. Farhood, N. Serbina, L. Huang, *Biochim. Biophys. Acta Biomembr.* **1995**, *1235*, 289 – 295.

[11] a) E. Liang, J. A. Hughes, *Biochim. Biophys. Acta Biomembr.* **1998**, *1369*, 39 – 50; b) A. Asokan, M. J. Cho, *Biochim. Biophys. Acta Biomembr.* **2003**, *1611*, 151 – 160; c) R. S. Singh, C. Goncalves, P. Sandrin, C. Pichon, P. Midoux, A. Chaudhuri, *Chem. Biol.* **2004**, *11*, 713 – 723; d) H. Hatakeyama, E. Ito, H. Akita, M. Oishi, Y. Nagasaki, S. Futaki, H. Harashima, *J. Controlled Release* **2009**, *139*, 127 – 132.

[12] a) E. Wagner, *Adv. Drug Delivery Rev.* **1999**, *38*, 279 – 289; b) N. Ferrer-Miralles, E. Vazquez, A. Villaverde, *Trends Biotechnol.* **2008**, *26*, 267 – 275.

[13] a) J.-P. Behr, *Tetrahedron Lett.* **1986**, *27*, 5861 – 5864; b) S. M. Mel'nikov, V. G. Sergeyev, K. Yoshikawa, *J. Am. Chem. Soc.* **1995**, *117*, 2401 – 2408; c) D. Llères, J.-M. Weibel, D. Heissler, G. Zuber, G. Duportail, Y. Mély, *J. Gene Med.* **2004**, *6*, 415 – 428; d) Y. Inoh, D. Kitamoto, N. Hirashima, M. Nakanishi, *J. Controlled Release* **2004**, *94*, 423 – 431; e) C. Bombelli, L. Giansanti, P. Luciani, G. Mancini, *Curr. Med. Chem.* **2009**, *16*, 171 – 183; f) W. X. Ding, T. Izumisawa, Y. Hattori, X. R. Qi, D. Kitamoto, Y. Maitani, *Biol. Pharm. Bull.* **2009**, *32*, 311 – 315.

[14] a) P. Pierrat, G. Creusat, G. Laverny, F. Pons, G. Zuber, L. Lebeau, *Chem. Eur. J.* **2012**, *18*, 3835 – 3839; b) P. Pierrat, G. Laverny, G. Creusat, P. Wehrung, J.-M. Strub, A. VanDorsselaer, F. Pons, G. Zuber, L. Lebeau, *Chem. Eur. J.* **2013**, *19*, 2344 – 2355.

[15] P. Pierrat, D. Kereselidze, P. Wehrung, G. Zuber, F. Pons, L. Lebeau, *Pharm. Res.* **2013**, *30*, 1362 – 1379.

[16] H. T. Lv, S. B. Zhang, B. Wang, S. H. Cui, J. Yan, *J. Controlled Release* **2006**, *114*, 100 – 109.

[17] S. S. Talmage, *Environmental and Human Safety of Major Surfactants – Alcohol Ethoxylates and Alkylphenol Ethoxylates*, CRC, Boca Raton, **1994**, p. 35.

[18] P. Pierrat, A. Casset, D. Kereselidze, M. Lux, F. Pons, L. Lebeau, *Macromol. Biosci.* **2016**, *16*, 984 – 989.

[19] a) J. M. Harris, E. C. Struck, M. G. Case, M. S. Paley, M. Yalpani, J. M. VanAlstine, D. E. Brooks, *J. Polym. Sci. Polym. Chem.* **1984**, *22*, 341 – 352; b) N. Boden, R. J. Bushby, S. Clarkson, S. D. Evans, P. F. Knowles, A. Marsh, *Tetrahedron* **1997**, *53*, 10939 – 10952; c) F. A. Loiseau, K. K. Hii, A. M. Hill, *J. Org. Chem.* **2004**, *69*, 639 – 647.

[20] P. Gentine, A. Bubel, C. Crucifix, L. Bourel-Bonnet, B. Frisch, *J. Liposome Res.* **2012**, *22*, 18 – 30.

[21] a) J. Ostergaard, C. Larsen, *Molecules* **2007**, *12*, 2396 – 2412; b) W. N. E. van Dijk-Wolthuis, M. J. van Steenbergen, W. J. M. Underberg, W. E. Hennink, *J. Pharm. Sci.* **1997**, *86*, 413 – 417.

[22] a) D. Maiolo, P. Del Pino, P. Metrangolo, W. J. Parak, F. B. Bombelli, *Nanomedicine* **2015**, *10*, 3231 – 3247; b) M. P. Monopoli, C. Aberg, A. Salvati, K. A. Dawson, *Nat. Nanotechnol.* **2012**, *7*, 779 – 786.

[23] a) T. Cedervall, I. Lynch, S. Lindman, T. Berggård, E. Thulin, H. Nilsson, K. A. Dawson, S. Linse, *Proc. Natl. Acad. Sci. USA* **2007**, *104*, 2050 – 2055; b) S. Gon, M. Bendersky, J. L. Ross, M. M. Santore, *Langmuir* **2010**, *26*, 12147 – 12154.

[24] G. Cevc, H. Richardsen, *Adv. Drug Delivery Rev.* **1999**, *38*, 207 – 232.

[25] R. Wattiaux, M. Jadot, M.-T. Warnier-Pirotte, S. Wattiaux-De Coninck, *FEBS Lett.* **1997**, *417*, 199 – 202.

[26] J. P. Clamme, S. Bernacchi, C. Vuilleumier, G. Duportail, Y. Mely, *Biochim. Biophys. Acta Biomembr.* **2000**, *1467*, 347 – 361.

[27] V. S. Trubetskoy, P. M. Slattum, J. E. Hagstrom, J. A. Wolff, V. G. Budker, *Anal. Biochem.* **1999**, *267*, 309 – 313.

[28] H. Akita, R. Ito, I. A. Khalil, S. Futaki, H. Harashima, *Mol. Ther.* **2004**, *9*, 443 – 451.

[29] G. Sahay, W. Querbes, C. Alabi, A. Eltoukhy, S. Sarkar, C. Zurenko, E. Karagiannis, K. Love, D. Chen, R. Zoncu, Y. Buganim, A. Schroeder, R. Langer, D. G. Anderson, *Nat. Biotechnol.* **2013**, *31*, 653-U119.

[30] www.who.int/respiratory/en, **2015**.

[31] D. C. Drummond, O. Meyer, K. L. Hong, D. B. Kirpotin, D. Papahadjopoulos, *Pharmacol. Rev.* **1999**, *51*, 691 – 743.

[32] a) K. A. Mislick, J. D. Baldeschwieler, *Proc. Natl. Acad. Sci. USA* **1996**, *93*, 12349 – 12354; b) L. Y. Song, Q. F. Ahkong, Q. Rong, Z. Wang, S. Ansell, M. J. Hope, B. Mui, *Biochim. Biophys. Acta Biomembr.* **2002**, *1558*, 1 – 13.

[33] B. Amulic, C. Cazalet, G. L. Hayes, K. D. Metzler, A. Zychlinsky, *Annu. Rev. Immunol.* **2012**, *30*, 459 – 489.

[34] L. Lebeau, S. Olland, P. Oudet, C. Mioskowski, *Chem. Phys. Lipids* **1992**, *62*, 93 – 103.

[35] M. A. Zanta, O. Boussif, A. Adib, J. P. Behr, *Bioconjugate Chem.* **1997**, *8*, 839 – 844.

[36] U. Griesenbach, C. C. Vicente, M. J. Roberts, C. X. Meng, S. Soussi, S. Xenariou, P. Tennant, A. Baker, E. Baker, C. Gordon, C. Vrettou, D. McCormick, R. Coles, A. M. Green, A. E. Lawton, S. G. Sumner-Jones, S. H. Cheng, R. K. Scheule, S. C. Hyde, D. R. Gill, D. D. Collie, G. McLachlan, E. Alton, *Biomaterials* **2011**, *32*, 2614 – 2624.

[37] a) Z. G. Dikmen, G. C. Gellert, S. Jackson, S. Gryaznov, R. Tressler, P. Dogan, W. E. Wright, J. W. Shay, *Cancer Res.* **2005**, *65*, 7866 – 7873; b) S. Foillard, G. Zuber, E. Doris, *Nanoscale* **2011**, *3*, 1461 – 1464.

[38] A. D. Edelstein, M. A. Tsuchida, N. Amodaj, H. Pinkard, R. D. Vale, N. Stuurman, *J. Biol. Methods* **2014**, *1*, e10.

Manuscript received: May 25, 2016

Accepted article published: July 5, 2016

Final article published: ■■ ▮▮, 0000

P. Pierrat, A. Casset, P. Didier,
*D. Kereselidze, M. Lux, F. Pons, L. Lebeau**

■■ – ■■

Cationic DOPC–Detergent Conjugates for Safe and Efficient in Vitro and in Vivo Nucleic Acid Delivery

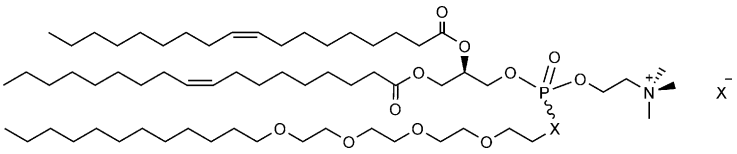

Pulmonary delivery: Biolabile DOPC–$C_{12}E_4$ conjugates were developed as nucleic acid carriers for in vitro and in vivo gene delivery. Their transfection efficiency and safety profile in mouse lung reflect their biodegradability and the surface active properties of the detergent released in situ. Thus, they might act as DNA carriers for gene therapy local administration through the airways.